Magnetostatic Wave Resonators Using Microstrip Disk

Makoto Tsutsumi, *Member, IEEE,* and Toshihito Umegaki

***Abstract*—We propose a magnetostatic wave resonator using yttrium iron garnet film with a microstrip disk. Assuming a magnetic wall at the edge of the disk, a dispersion relation is derived and solved numerically to obtain the resonant frequency. Resonant mode charts are given for various parameters of resonator. The quality factor is also given as a function of the resonator dimensions. Resonant characteristics are confirmed experimentally using 40 μm and 13.5 μm thick YIG films with 5 mm diameter strip disk at *S* band.**

I. Introduction

MANY types of magnetostatic wave resonators using yttrium iron garnet (YIG) films have been reported extensively [1]. For rectangular shape resonators the straight edge resonant mode has been studied [2]. Another type of the straight edge mode excited by a comb transducer has been studied to obtain low insertion loss [3]. For disk shaped resonators, uniform precession mode excited by two orthogonal microstrips has been investigated to achieve high quality factor [4]. Recently magnetostatic wave resonator of microstrip disk type has been proposed, but insertion loss was high of more than 10 dB [5].

This paper treats magnetostatic wave resonator of microstrip disk type of low insertion loss. Assuming magnetic wall at the edge of the microstrip disk resonant mode charts were calculated for various resonator parameters. Characteristics of the resonator were confirmed experimentally at *S* band.

II. Analysis

A cross section of the microstrip resonator is shown in Fig. 1. A microstrip disk having radius a is bonded on the YIG film of thickness b epitaxially grown on gadolinium gallium garnet (GGG) substrate of thickness w. Bias magnetic field $\mu_0 H_0$ is applied perpendicular to the YIG film.

From magnetostatic approximation:

$$\nabla \times \boldsymbol{H} = 0, \quad \nabla \cdot \boldsymbol{B} = 0.$$

The scalar magnetic potential ψ in the YIG film from $\boldsymbol{H} = -\nabla\psi$ satisfies the differential equation

Manuscript received July 16, 1991; revised December 11, 1991. This work was partially supported by the 1990 Japanese Broadcasting Foundation.

The authors are with the Department of Electronics, and Information Science, Kyoto Institute of Technology, Sakyo Ku Matsugasaki, Kyoto 606, Japan.

IEEE Log Number 9106769.

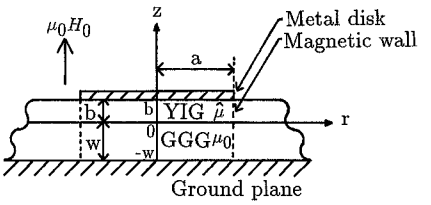

Fig. 1. Geometry of the problem.

$$\mu\left\{\frac{1}{r}\frac{\partial}{\partial r}\left(r\frac{\partial\psi}{\partial r}\right)+\frac{1}{r^2}\frac{\partial^2\psi}{\partial\theta^2}\right\}+\frac{\partial^2\psi}{\partial z^2}=0, \tag{1}$$

where μ is the diagonal component of permeability tensor of the YIG.

The solution of (1) is expressed as

$$\psi = AJ_m(k_c r)e^{-jm\theta}\cos k_z(z-b), \tag{2}$$

where A is an arbitrary constant, phase constant k_z is given by

$$k_z = \sqrt{-\mu}\,k_c.$$

Equation (2) satisfies zero normal component of magnetic flux density to microstrip disk at $z = b$.

A magnetic wall at $r = a$ is assumed. Hence the phase constant k_c is given by

$$k_c = \frac{y_{m\tilde{n}}}{a},$$

where $y_{m\tilde{n}}$ is the $\tilde{n}$th root of Bessel function of mth order. Boundary condition on the magnetic wall around the metal disk has been assumed to analyze electromagnetic field in the ferrite media [6], but it has not been used for magnetostatic wave problem and for magnetostatic potential variation in the z direction.

The magnetic potential ϕ in the GGG satisfies the differential equation

$$\frac{1}{r}\frac{\partial}{\partial r}\left(r\frac{\partial\phi}{\partial r}\right)+\frac{1}{r^2}\frac{\partial^2\phi}{\partial\theta^2}+\frac{\partial^2\phi}{\partial z^2}=0, \tag{3}$$

the solution of (3) is expressed as

$$\phi = BJ_m(k_c r)e^{-jm\theta}\cosh k_c(z+w). \tag{4}$$

Equation (4) satisfies zero normal component of magnetic flux density at $z = -w$.

The magnetic potentials (2), (4) and normal component of magnetic flux densities in the YIG and in the GGG are matched at the interface $z = 0$. These boundary condi-

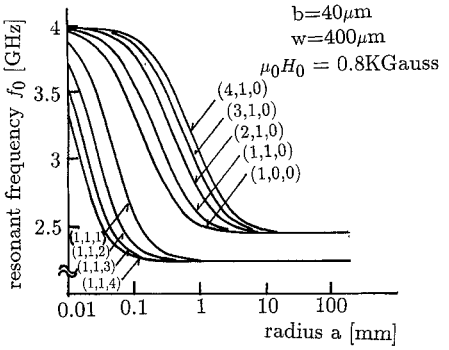

Fig. 2. Resonant mode chart as a function of radius a.

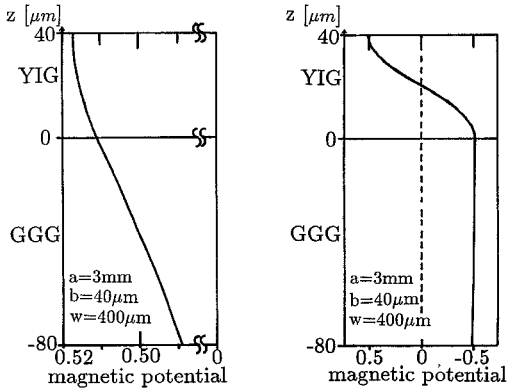

Fig. 3. Magnetic potential distributions in the YIG film. (a) (1, 1, 0) mode. (b) (1, 1, 1) mode.

tions lead to dispersion relation

$$k_z \tan (k_z b - n\pi) = k_c \tanh (k_c w), \tag{5}$$

where n is integer.

Fig. 2 shows resonant mode chart as a function of radius a for various mode number where b and w are 40 μm and 400 μm, respectively. Modes are characterized by three integers ($\tilde{n}$, m, n) which signify the mode numbers in the r, θ, and z directions, respectively.

We define the resonant mode whose magnetic potential varies exponentially in the direction of the bias magnetic field as the (1, 1, 0) mode, as shown in Fig. 3(a). The RF magnetic field H_z of (1, 1, 0) mode is bounded tightly to the interface between the YIG film and the GGG substrate. In Fig. 2, the (1, 0, 0) mode is fundamental and is independent of circular θ direction. It seems to be difficult to excite (1, 0, 0) mode by the antenna configuration discussed in Section III, hence the second resonant (1, 1, 0) mode is considered in our numerical calculation. While the magnetic potential for (1, 1, 1) mode confines only in the YIG film with sinusoidal distribution as shown in Fig. 3(b).

Fig. 4 shows resonant frequency for two modes (1, 1, 0) and (1, 1, 1) as a function of the radius a for different GGG thicknesses where b is 40 μm. Strong dependence of resonant frequency on GGG thickness is found for (1, 1, 0) mode while for (1, 1, 1) mode, it is not sensitive for resonator geometries.

Fig. 5 shows the resonant frequency for (1, 1, 0) and (1, 1, 1) modes as a function of radius a for various values of YIG film thicknesses where w is 400 μm.

The rf magnetic field distribution within microstrip disk is also calculated at $z \simeq b$ for (1, 1, 0) mode as shown in Fig. 6. It can be seen that the rf field is confined in the center of disk.

The quality factor of the microstrip resonator consists of two factors. One is the quality factor due to the material loss as defined by

$$Q_{\Delta H} = \frac{2\pi f_0}{\gamma \mu_0 \Delta H}, \tag{6}$$

where f_0 is the resonant frequency, and ΔH is the linewidth of the ferrimagnetic resonance of the YIG film, which is about 1 Oe for commercial available YIG film.

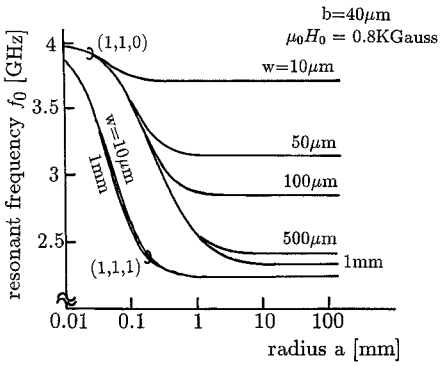

Fig. 4. Resonant frequency of (1, 1, 0) and (1, 1, 1) modes for different GGG thicknesses.

Second is the quality factor Q_M defined by the dissipated energies ($P_{d1} + P_{d2}$), where P_{d1} and P_{d2} are those due to the surface resistivity of the microstrip disk and ground plane, respectively, and can be expressed as

$$Q_M = \frac{2\pi f_0}{P_{d1} + P_{d2}} (U_1 + U_2),$$

$$U_1 = \tfrac{1}{2} \mu_0 \int_v \frac{\partial \hat{\mu} \omega}{\partial \omega} \boldsymbol{H_1} \cdot \boldsymbol{H_1^*}\, \boldsymbol{dv},$$

$$U_2 = \tfrac{1}{2} \mu_0 \int_v \boldsymbol{H_2} \cdot \boldsymbol{H_2^*}\, \boldsymbol{dv},$$

$$P_{d1} = \tfrac{1}{2} \int_s R_s \boldsymbol{H_{t1}} \cdot \boldsymbol{H_{t1}^*}\, \boldsymbol{ds},$$

$$P_{d2} = \tfrac{1}{2} \int_s R_s \boldsymbol{H_{t2}} \cdot \boldsymbol{H_{t2}^*}\, \boldsymbol{ds}, \tag{7}$$

where U_1 and U_2 are the stored energies in the YIG film and the GGG substrate, respectively, $\hat{\mu}$ is the permeability tensor of the YIG film, H_{t1} and H_{t2} are the peak values of the tangential magnetic field in the YIG film and GGG substrate, respectively, and R_s is the surface resistivity.

Total quality factor is defined by the sum of two factors:

$$\frac{1}{Q} = \frac{1}{Q_{\Delta H}} + \frac{1}{Q_M}.$$

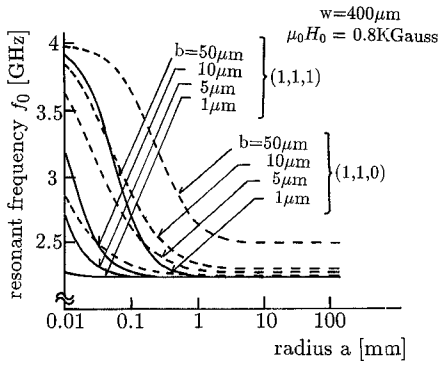

Fig. 5. Resonant frequency of (1, 1, 0) and (1, 1, 1) modes for different YIG thicknesses.

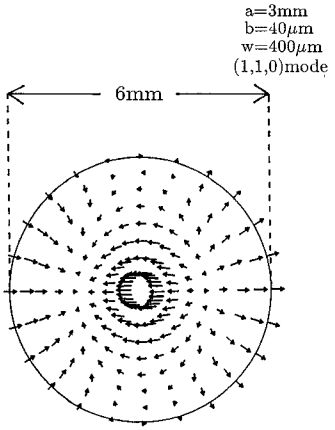

Fig. 6. RF field distribution in the microstrip disk.

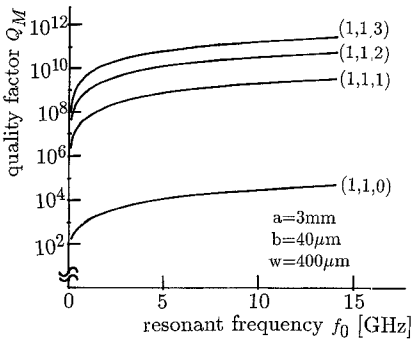

Fig. 7. Quality factor of metal disk for different modes as a function of resonant frequency.

The Q_M is evaluated numerically from (7), and is shown in Fig. 7 as a function of resonant frequency and for various mode numbers. The surface resistivity R_s is assumed to be $2.61 \times 10^{-7}\sqrt{f_0}\ \Omega$ for copper. The quality factor Q_M is higher for higher order modes. From the numerically estimated results shown in figures 4 and 5, it is found that the resonant mode (1, 1, 0) depends strongly on the dimension of metal disk which may reduce the quality factor. However it can be seen from Fig. 7 that (1, 1, 0) mode possesses high quality factor over 10^4 beyond 5 GHz. Hence the quality factor of resonator is governed mainly by the material loss rather than the metallic loss.

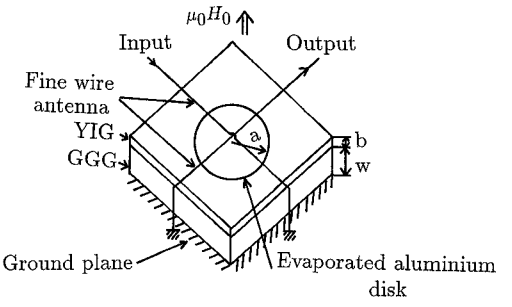

Fig. 8. Microstrip disk resonator using YIG film substrate.

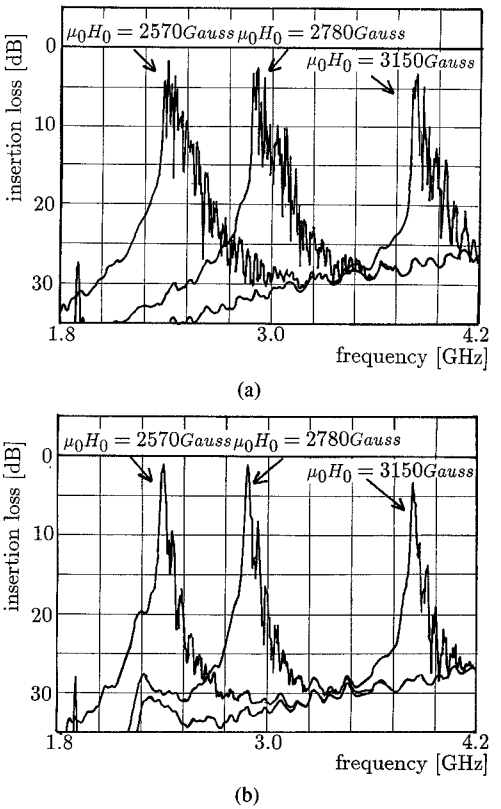

Fig. 9. Measured resonant frequency for various bias magnetic fields. (a) Without disk. (b) With disk.

III. Experiments

The structure of the resonator consists of a microstrip disk placed on the center of a YIG film as shown in Fig. 8. The YIG film dimension is $9.5 \times 9.5\ mm^2$. Bias magnetic field is applied perpendicularly to the YIG film. Two orthogonal coupled fine wire antennas of diameter of 200 μm were used to excite magnetostatic wave to the microstrip disk as shown in figure. Each wire antenna is insulated by 10 μm thick mica film. Several resonators were fabricated and tested with different radii for the disk.

To confirm the effect of metal disk on resonance behavior, the characteristics of resonator without disk are investigated first. Its typical frequency response is shown in Fig. 9(a) for different bias magnetic fields with 40 μm thick YIG film on 400 μm GGG substrate. Resonant behavior is resulted by the reflection of magnetostatic waves from the edges of rectangular YIG sample. Next a mi-

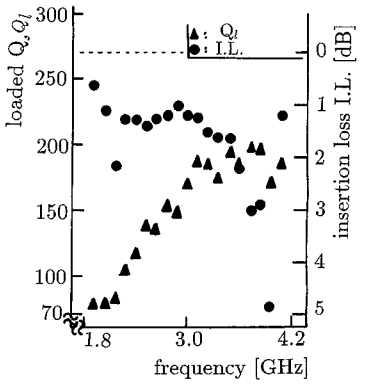

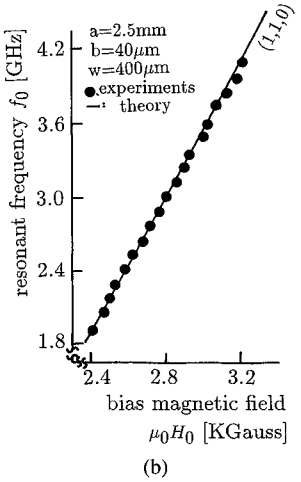

Fig. 10. Measured resonator characteristics as a function of frequency. (a) Insertion loss and loaded Q. (b) Resonant frequency.

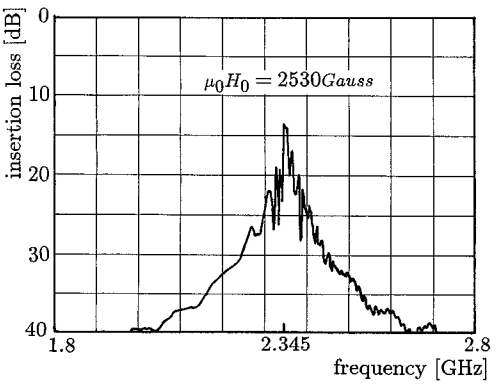

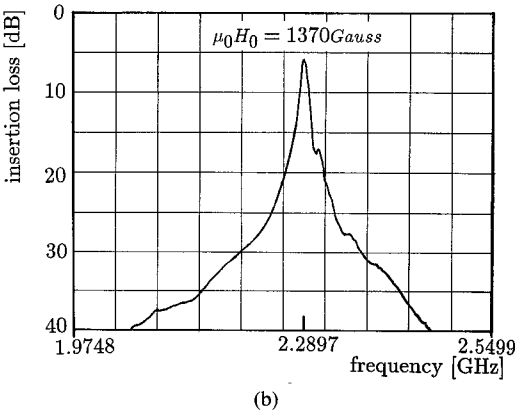

Fig. 11. Measured resonant frequency of resonator with YIG film disk substrate. (a) Without microstrip disk. (b) With microstrip disk.

crostrip disk of Aluminum with 2 μm thick and diameter of 5 mm is evaporated on the same YIG sample. Its frequency response is shown in Fig. 9(b) for different bias magnetic fields.

By comparing the results of Fig. 9(a) and (b), it is found that the large ripples appeared in Fig. 9(a) are suppressed by the presence of aluminum disk and by the confinement of magnetostatic wave energy within the disk.

In Fig. 9(b) resonant characteristic with average insertion loss of few dBs is observed with maximum off resonance rejection of 25 dB. The input antenna is arranged orthogonal to the output antenna as shown in Fig. 8. In such antenna configurations, RF field from the source distributes inhomogeneously in the circular θ direction. Therefore observed resonance mode of Fig. 9(b) will be the (1, m, 0) and $m = 1$ mode is considered because higher order modes $m \geq 2$ were insensitive for microstrip disk dimensions.

From point of view of comparison between theory of Fig. 2 and experiment, small ripples of resonant characteristics of Fig. 9(b) may be due to excitation of the adjacent higher resonant mode and to the weak concentration of RF energy of (1, 1, 0) mode within microstrip disk.

The bias magnetic field dependence of resonator on the loaded Q_l, insertion loss I.L. and resonant frequency were measured ranging from 1.8 GHz to 4.2 GHz and shown in Fig. 10. Minimum insertion loss of 0.6 dB near 1.8 GHz is observed in Fig. 10(a) and it may be attribute to a good impedance matching of the RF source. Maximum Q_l of 200 is measured at 4 GHz, which is lower than theoretically estimated Q value. Reduction of quality factor will be caused by the tight coupling between input, output wire transducers and resonator. Fig. 10(b) shows resonant frequency versus magnetic field. Theoretical value of (1, 1, 0) mode is also depicted in the figure, which take into account of demagnetizing field about 1810 Gauss. It can be seen that resonant frequency changes according to the relation of 2.8 MHz $\cdot$ $\mu_0 H_0$, where $\mu_0 H_0$ is the bias magnetic field.

An additional experiment on resonator was carried out using 13.5 μm thick YIG film disk having diameter of 9.5 mm and 6 mm diameter strip disk. The result is shown in Fig. 11. Ripples due to film edge is found to be considerably reduced compared to the rectangular YIG film substrate of 40 μm thickness. But insertion loss is slightly high as shown in Fig. 11(b).

IV. Conclusion

Characteristics of the magnetostatic wave resonators using microstrip disk have been analyzed by modeling the magnetic wall around the disk edge. Mode chart for various resonator dimensions have been given and quality factor has also been calculated.

Experiments were carried out using rectangular 40 μm thick YIG film substrate with 5 mm diameter microstrip disk and 13.5 μm thick YIG film disk substrate with 6 mm strip disk. Typical resonant characteristics reveal loaded $Q_l = 200$ at 4 GHz, average insertion loss of 1.5 dB and dynamic range of 25 dB. These experimental results were discussed with theory.

If we adjust YIG film and disk dimensions, and by changing the thickness of GGG, further improvement of the resonant characteristics are possible with high dynamic range.

References

[1] "Special section on microwave magnetics," *Proc. IEEE*, vol. 76, no. 2, pp. 121–200, Feb. 1988.

[2] W. Ishak and K. W. Chang, "Tunable microwave resonators using magnetostatic wave in YIG film," *IEEE Trans. Microwave Theory Tech.*, MTT-34, no. 12, pp. 1383–1393, Dec. 1986.

[3] Y. Kinoshita, S. Kubota, S. Takeda, and A. Nakagoshi, "Planar resonator and integrated oscillator using magnetostatic waves," *IEEE Trans. Ultrason., Ferroelec., Freq. Contr.*, vol. 37, no. 5, pp. 457–463, Sept. 1990.

[4] Y. Murakami, T. Ohgihara, and T. Okamoto, "A 0.5–4.0 GHz tunable bandpass filter using YIG film grown by LPE," *IEEE Trans. Microwave Theory and Tech.*, vol. MTT-35, no. 12, pp. 1192–1198, Dec. 1987.

[5] M. Tsutsumi and T. Takeda, "Magnetostatic wave resonators of microstrip type," in *1989 IEEE MTT-S Int. Microwave Symp. Dig.*, pp. 149–152.

[6] A. Khilla and I. Wolff, "The point matching solution for magnetically tunable cylindrical cavities and ferrite planar resonators," *IEEE Trans. Microwave Theory Tech.*, vol. MTT-27, no. 6, pp. 592–598, June 1979.

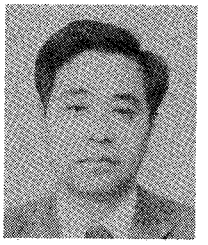

Makoto Tsutsumi (M'71) was born in Tokyo Japan, on February 25, 1937. He received the B.S. degree in electrical engineering from Ritsumeikan University, Kyoto, Japan, in 1961 and the M.S. and Ph.D. degrees in communciation engineering from Osaka University, Osaka, Japan, in 1963 and 1971, respectively.

From 1984 to 1987 he was an Associate Professor of Communication Engineering at Osaka University. Since 1988 he has been a Professor at the Kyoto Institute of Technology, Department of Electronics and Information Science, Kyoto, Japan. His research interests are primarily in microwave and millimeter-wave ferrite devices and optics/microwave interactions.

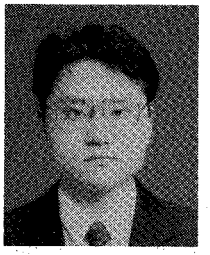

Toshihito Umegaki was born in Osaka, Japan, on July 12, 1968. He received the B.E. degree in electrical engineering from Kyoto Institute of Technology, Kyoto, Japan, in 1991. Currently, he is studying toward the M.E. degree at the same university.

His current interests are in the microwave filters using YIG films.